JOURNAL OF MATERIALS SCIENCE: MATERIALS IN MEDICINE **13** (2002) 1057–1063

Micrometer level structural and chemical evaluation of electrodeposited calcium phosphate coatings on TA6V substrate by STEM-EDXS

H. BENHAYOUNE, P. LAQUERRIERE, E. JALLOT, A. PERCHET, L. KILIAN,
G. BALOSSIER
INSERM-ERM 0203, Laboratoire de Microscopie Electronique, 21, rue Clément Ader, 51685 Reims BP 138 Cedex 02, France

J. L. BUBENDORFF
Laboratoire de Microscopie Electronique et Tunnel, 21, rue Clément Ader, 51685 Reims BP 138 Cedex 02, France

G. D. SOCKALINGUM
Unité MéDIAN, CNRS FRE 2141, UFR de Pharmacie, 51 rue Cognacq-Jay, 51096 Reims Cedex

Hydroxyapatite (HA) coatings on titanium alloy substrates Ti6Al4V have been prepared in our laboratory by electrodeposition and hydrothermal synthesis. In this paper, the morphology, crystal size, porosity and Ca/P atomic ratio are investigated using scanning electron microscopy (SEM), scanning transmission electron microscopy (STEM), Raman microspectroscopy and X-ray energy dispersive spectroscopy (EDXS). The results obtained show that after being hydrothermally treated and calcined at high temperature, the electrodeposited brushite coating is converted into a stoichiometric hydroxyapatite having a crystal size which changes considerably from the surface to the substrate alloy. In addition, variation of the surface coating porosity as a function of the electrolyte temperature has also been carried out.

1. Introduction

Most orthopedic materials in current use are generally titanium and its alloys. In an attempt to enhance the biocompatibility of these kinds of materials, they are often coated with osteointegrating and/or osteoconductive biomaterials such as calcium phosphate ceramics. Among these biomaterials, hydroxyapatite (HA) seems to have been the most investigated biomaterial during the last 12 years. Currently, the plasma spray technique is extensively used by the implant industry to deposit hydroxyapatite on metallic substrates. However, this technique requires HA powders in pure form which may be relatively expensive and involves high temperatures leading to the formation of easily dissolved phases such as amorphous HA [1, 2].

Presently, a technique based on electrodeposition is used for coating HA at relatively low temperatures without use of any kind of HA powders [3, 4]. The process is, in general, composed of two steps: electrodeposition of a calcium phosphate using electrolyte made by mixing solutions containing calcium and phosphorous, and conversion of this coating to HA by specific treatments. Therefore, it is very important to study the effects of the electrodeposition and/or treatment parameters on the structure and the composition of the coating obtained.

The aim of the present work is to analyze at a micrometer scale, calcium phosphate coatings on titanium alloys elaborated in our laboratory by electrodeposition. The analysis is made by scanning transmission electron microscopy (STEM) associated to X-ray energy dispersive spectroscopy (EDXS). Such techniques require a special specimen preparation which is performed in our laboratory. Furthermore, scanning electron microscopy (SEM) and Raman microspectroscopy were also used for morphology and phase composition study of the calcium phosphate coatings.

2. Experimental procedures

2.1. Sample characteristics

The substrates were mechanically grounded Ti6Al4V discs with a diameter of 10 mm and a thickness of 2 mm. Brushite coatings on Ti6Al4V were prepared by electrodeposition following the method described by Shirkhanzadeh [5]. The electrolyte (Fig. 1) used was made by mixing 0.042 M $Ca(NO_3)_2 \cdot 4H_2O$ and 0.125 M $NH_4H_2PO_4$ solutions. The pH value of the electrolyte was adjusted to 4 by adding nitric acid. The coating process was carried out at 65 °C under N_2 atmosphere and $E_c = -1.6$ V cathode potential (versus SCE reference electrode) for 60 min. Two graphite rods acting as

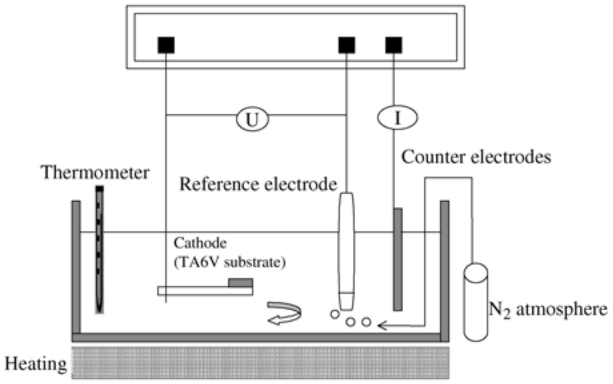

Figure 1 Schematic view of the electrolyte used to prepare brushite coatings.

counter electrodes were used, and the electrodeposition was accomplished using a potentiostat/galvanostat operating in potentiostatic mode by varying current density.

The brushite coatings obtained were then hydrothermally treated at 125 °C and pH = 7 in an autoclave (Fig. 2) for 4 h and finally calcined at 425 °C for 6 h to convert into hydroxyapatite (HA) coatings.

2.2. Scanning electron microscopy (SEM)

The morphology of coatings was observed in secondary electron mode using a field effect electron microscope LEO; the primary beam energy was 3 keV with a primary beam current close to 5 μA.

2.3. Raman microspectroscopy

Confocal Raman microspectroscopy has been applied on the coating using a Labram microspectrometer (Dilor, Jobin-Yvon, Horiba, France). This spectrometer is equipped with a He/Ne laser delivering a power of 2 mW at the sample, an illumination optical unit, which permits a good illumination of the sample by the laser light, an optical microscope (high stability BX 40 Olympus 100 × (NA 0.9) objective) was used, a collection optical unit, which takes into account the confocal hole. It is also composed of a dispersive system composed of two gratings mounted on the same shaft 1800 grooves/mm (holographic) and 600 grooves/mm (ruled and holographic) and a multichannel CCD detector of 1024 × 256 pixels. The spectral resolution depends on the slit size; for usual experimental conditions, the spectral resolution was about 6 cm^{-1} and the spatial resolution was about 1 μm.

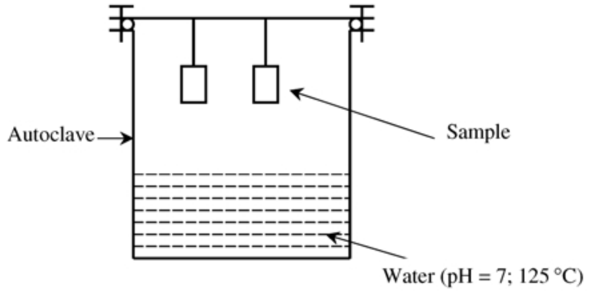

Figure 2 Schematic representation of the apparatus for hydrothermal treatment.

Spectral treatment is sometimes necessary to reveal vibrational or structural information. All the different mathematical operations (baseline correction, subtraction, smoothing) were performed using the Labspec software(Dilor, Jobin-Yvon, Horiba, France).

2.4. Scanning transmission electron microscopy

For STEM observation, the specimens were embedded in a resin. Thick sections were made perpendicular to the TA6V substrate using a low-speed diamond saw and polished in order to achieve a plane surface. The alloy substrate was carefully removed from the half-sections. At this stage, the samples were only calcium phosphate embedded in resin. Finally, ultrathin sections (~ 100 nm) were cut with a diamond knife using an ultramicrotome and collected on copper grids. The sections were coated with a conductive layer of carbon in a sputter coater to avoid charging effects. They were observed using a scanning transmission microscope STEM (Philips CM30) operating at a voltage of 100 kV. X-ray analysis was performed using energy dispersion X-ray spectroscopy EDXS. The detector was an Si(Li) diode equipped with an ultrathin window. The quantitative analysis of X-ray spectra was made using a quantification program based on the Hall method [6] and performed in our laboratory [7].

3. Results and discussion

3.1. Morphology and mineral species evaluation

The SEM micrograph of Fig. 3 shows the morphology of the electrodeposited coating. It consists mostly of brushite ($CaHPO_4 \cdot 2H_2O$) composed of fine grains and having a microporous structure. The dimensions of the micropores present in the coating range from 1 to 2 μm.

After the hydrothermal treatment, the coating presents thin needle-like crystals with the length having an average value of 1 μm (Fig. 4). The structure is

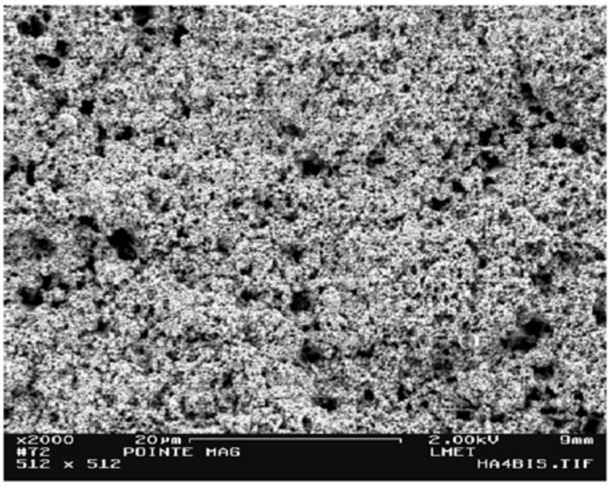

Figure 3 Secondary electrons micrograph of the electrodeposited coating (magnification 2000 ×).

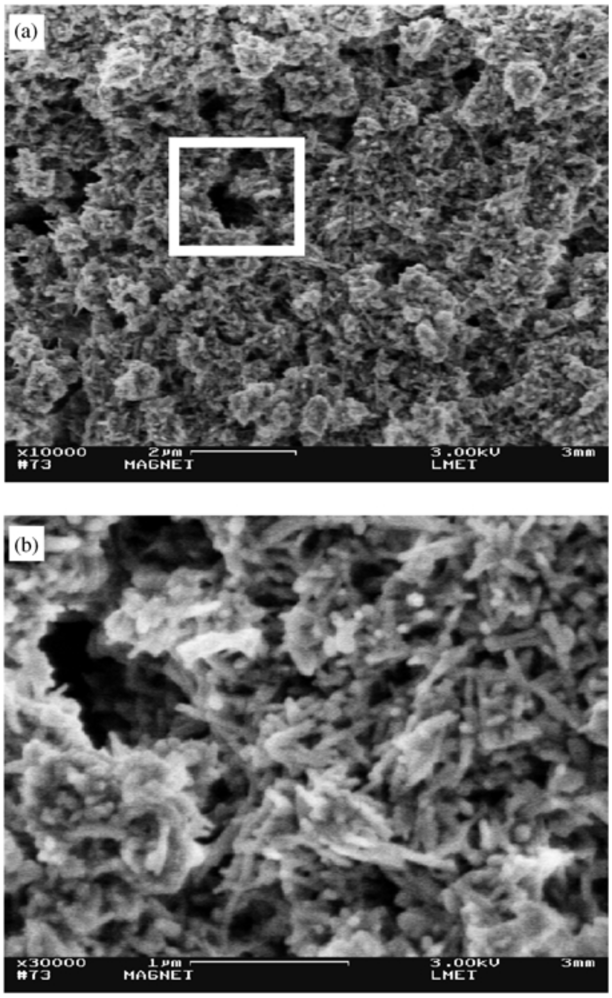

Figure 4 Secondary electrons micrograph of the electrodeposited coating after hydrothermal treatment: (a) magnification 10 000 × (b) magnification 30 000 × (selected area of Fig. 4(a)).

microporous and the dimensions of the micropores are the same as the brushite coating.

Fig. 5 represents the Raman spectra recorded on the brushite coating before and after hydrothermal treatment. It clearly shows that after hydrothermal treatment, the coating spectrum presents a high background due to fluorescence. This phenomenon has been observed already when a plasma sprayed hydroxyapatite coating was investigated by Raman spectroscopy [8].

Fig. 6 represents the same spectra after fluorescence subtraction. The brushite spectrum is made of peaks at 434, 450, 592, 613, 720, 741, 960, 1008, 1050 and 1453 cm^{-1}. The peaks at 434, 450, 592, 613, 960 and 1008 cm^{-1} are due to the PO_4^{3-} group vibrations. The other peaks are due to CO_3^{2-} group vibrations according to Nakamoto [9]. The carbonate group vibration is probably due to $CaCO_3$ groups that are incorporated in the coating during the electrodeposition process by precipitation.

After hydrothermal treatment, the spectrum exhibits peaks corresponding to PO_4^{3-} groups and a very weak CO_3^{2-} band indicating that the carbonate quantity decreases after hydrothermal treatment.

Fig. 7, represents the spectra obtained on the brushite coating before and after hydrothermal treatment in the same conditions as spectra of Fig. 5 but in the range of 3520–3620 cm^{-1}. The peaks observed at 3568 cm^{-1} before treatment and at 3572 cm^{-1} after treatment correspond to the vibration of the OH^- groups. The shift between the two peaks is characteristic of lattice reorganization during the treatment.

Such results imply that the coating obtained is stoichiometric hydroxyapatite following. Han *et al.* [10] when using X-ray diffractometry and infrared spectroscopy for brushite coating characterization at variable hydrothermal treatment parameters.

3.2. Structural and chemical analysis at micrometer scale

STEM micrographs of the sections show a part of the calcium phosphate coating (about 10 μm thick) in contact with the resin (Fig. 8(a)). They clearly reveal a variation of the crystal size in the coating. Indeed, in the vicinity of the coating/resin interface, which corresponds to the coating surface observed in SEM, the crystal size is about

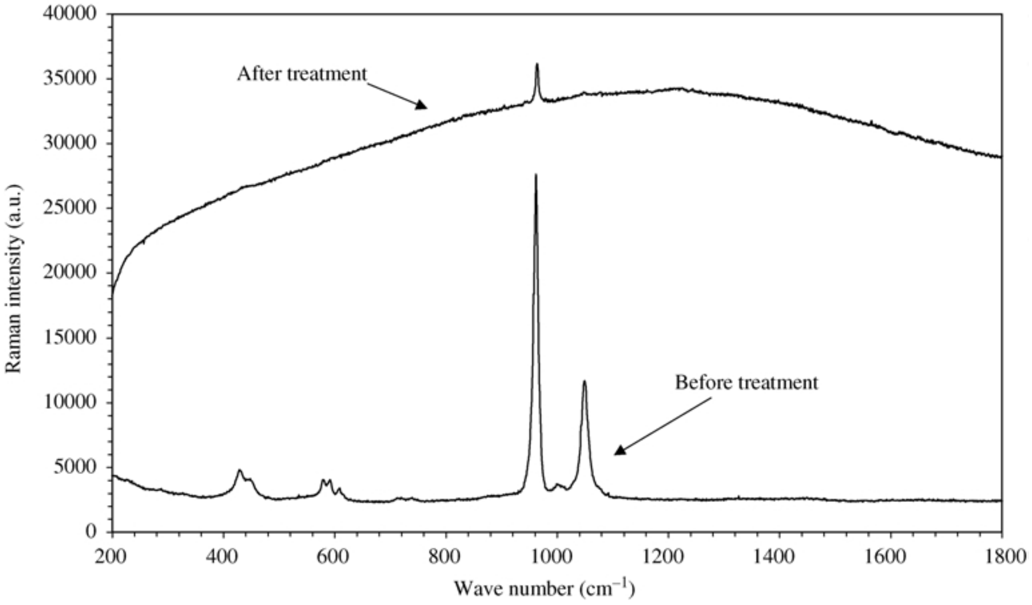

Figure 5 Raman spectra of the electrodeposited coating before and after hydrothermal treatment (10 accumulations of 50 s at 6 cm^{-1} resolution).

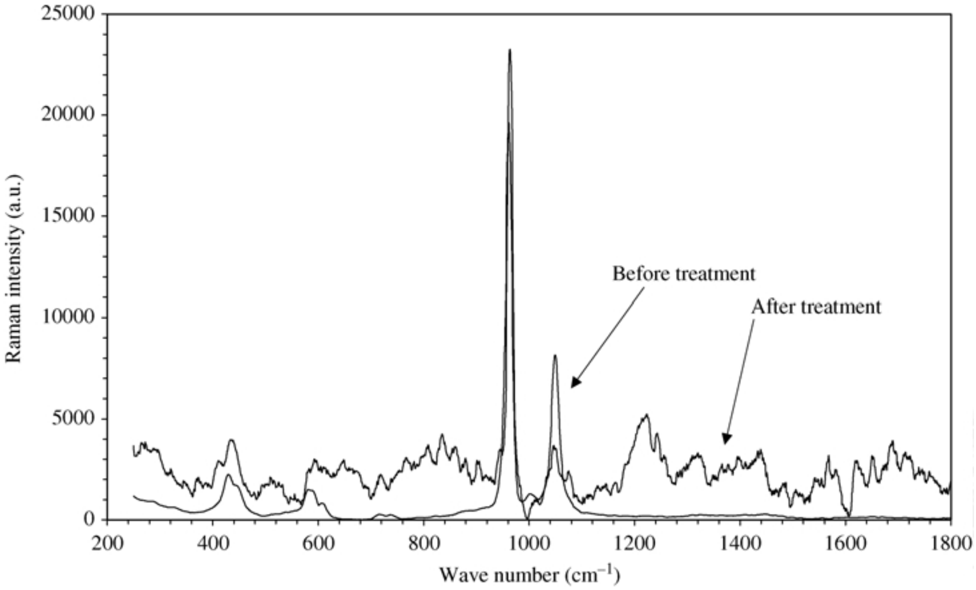

Figure 6 Raman spectra subtracted of background fluorescence of the electrodeposited coating before and after hydrothermal treatment (10 accumulations of 50 s at 6 cm^{-1} resolution).

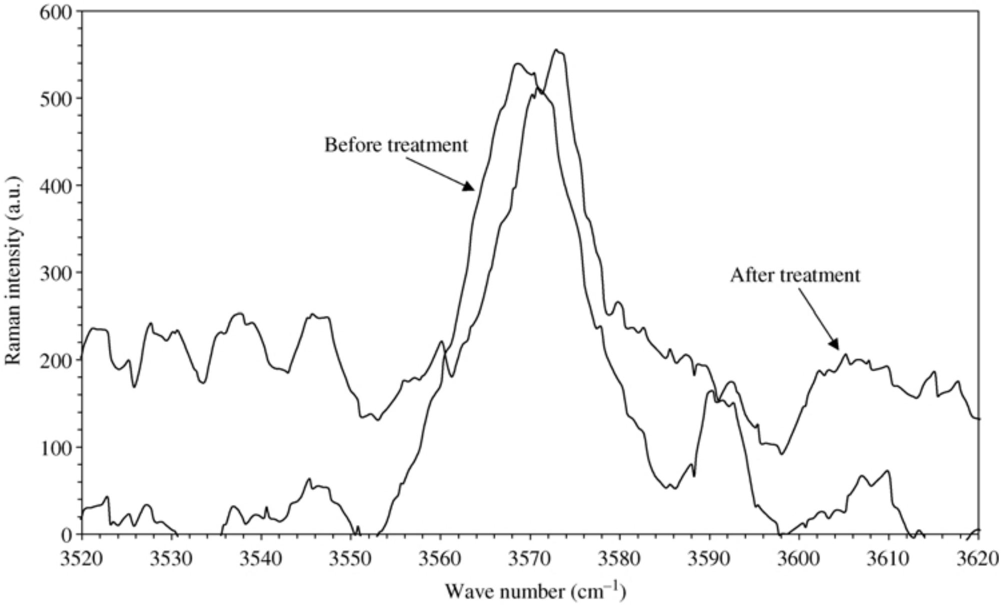

Figure 7 Raman spectra of the electrodeposited coating showing OH$^-$ vibration before and after hydrothermal treatment (10 accumulations of 50 s at 6 cm^{-1} resolution).

75 nm in diameter (Fig. 8(b) and (d)). But near the coating/TA6V substrate interface, the crystal size increases and may reach 300 nm in diameter (Fig. 8(c) and (e)). This crystal size variation is very interesting since it is particularly desirable for better chemical interaction with the biological environment [11].

On the other hand, Ca/P atomic concentration ratio profile of the coating was obtained from X-ray intensity measurements using energy dispersive X-ray spectroscopy (Fig. 9). The scan line of about 5 μm with 0.5 μm step starts near the coating/TA6V substrate interface and ends near the coating/resin interface (see dashed line on Fig. 8(a)). The results show that the Ca/P ratio is relatively constant along the profile; the mean value within the coating is about 1.71 ± 0.04. This value seems to confirm the prediction deduced from Raman spectroscopic data which suppose that the converting coating after hydrothermal treatment is a stoichiometric hydroxyapatite.

3.3. Influence of the electrolyte temperature on the surface coating porosity

In order to evaluate the influence of the electrolyte temperature on the surface coating porosity, HA coatings have been electrodeposited at two different electrolyte temperatures of 40 and 65 °C. The SEM micrograph of the coating at 40 °C is shown in Fig. 10(a). Comparison with the SEM micrograph of the coating at 65 °C (Fig. 10(b)) shows that the HA coating at 40 °C temperature

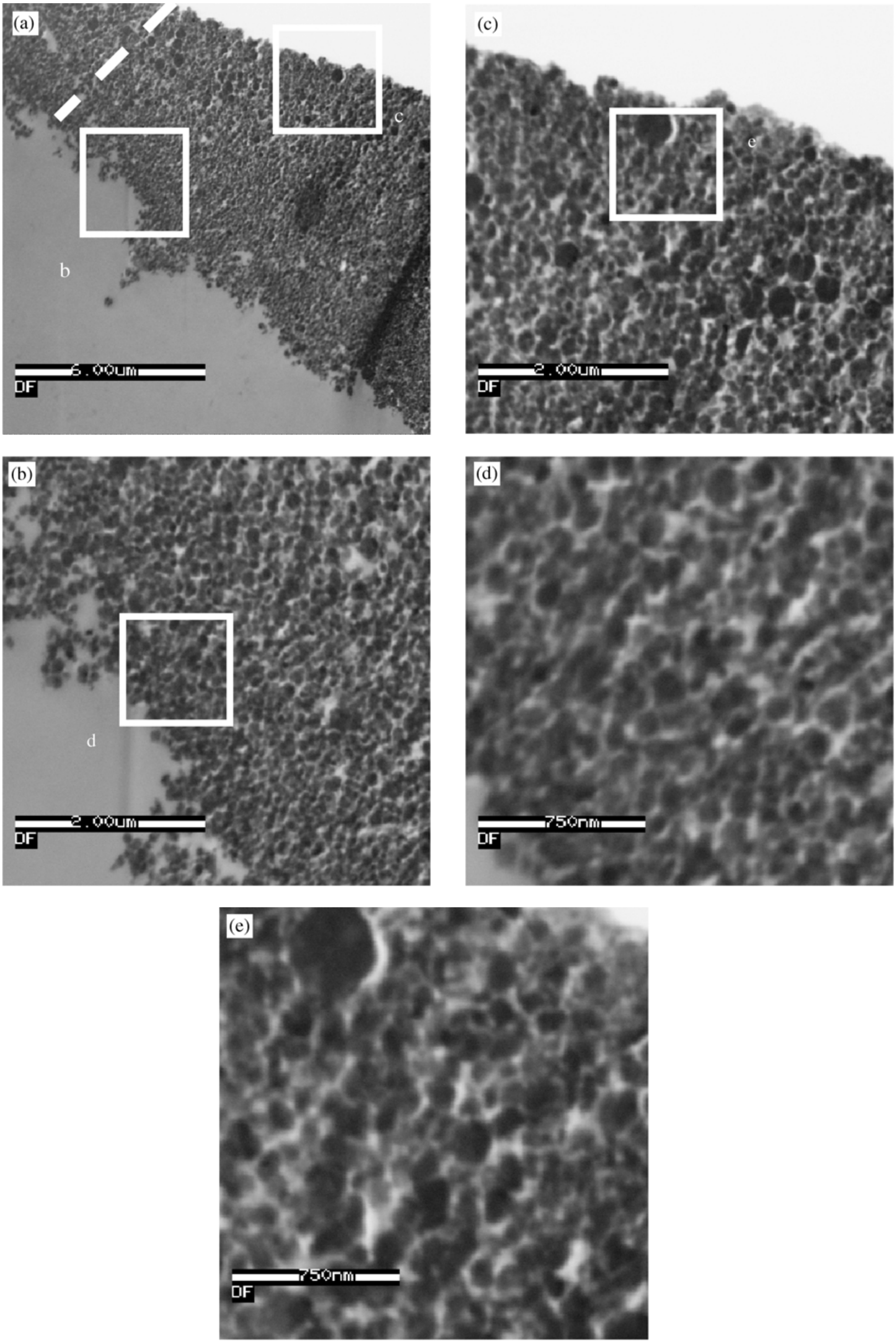

Figure 8 Scanning transmission microscopy micrograph showing (a) global view of ultrathin section of the coating embedded in resin (magnification 10 000 ×); (b) selected area (b) on Fig. 8(a), coating/resin interface (magnification 30 000 ×); (c) selected area (c) on Fig. 8(a), coating/TA6V substrate interface (magnification 30 000 ×), (d) selected area (d) on Fig. 8(b), crystal of weak size near the coating/resin interface (magnification 70 000 ×); (e) selected area (e) on Fig. 8(c), crystal of high size near the coating/TA6V substrate interface (magnification 70 000 ×).

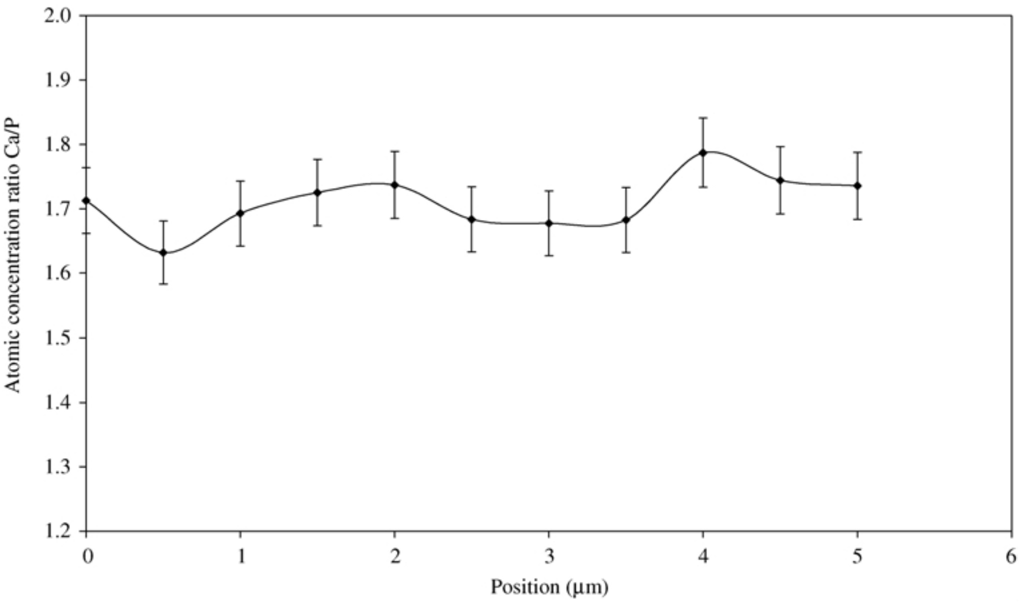

Figure 9 Atomic concentration ratio Ca/P profile across the coating.

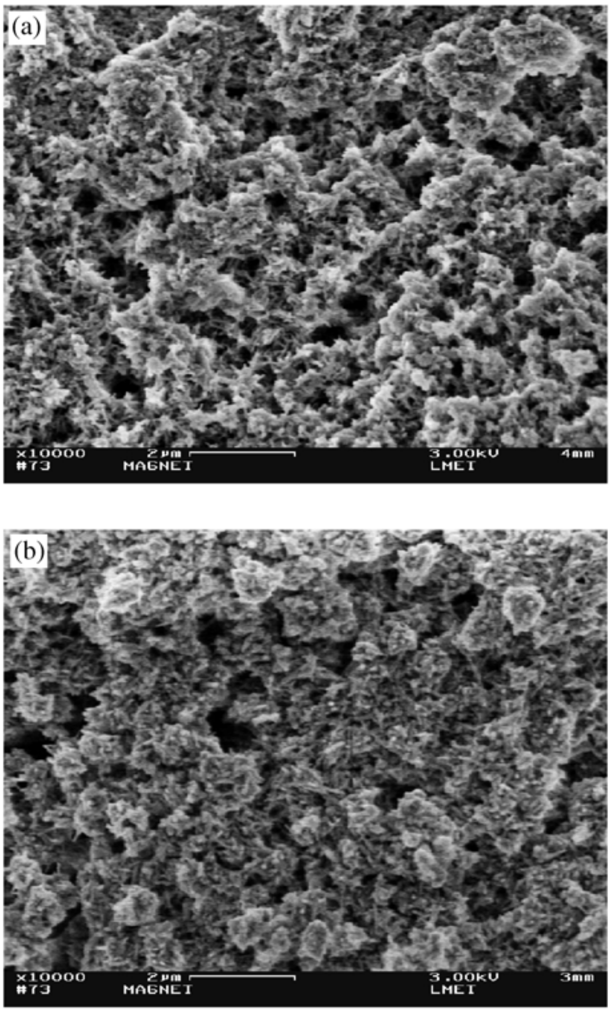

Figure 10 Secondary electron micrograph showing (a) the coating electrodeposited with the electrolyte at 40 °C; (b) the coating electrodeposited with the electrolyte at 65 °C.

has a higher microporosity than the coating at 65 °C. This indicates that the electrodeposited brushite coating becomes more compact when increasing the electrolyte temperature is increased. Similar results have been observed by Han *et al.* [12] by varying the current density instead of the temperature. This suggests that HA coating of gradient porosity may be realized by gradually varying the electrolyte temperature.

4. Conclusion

In this study, a structural and chemical evaluation of stoichiometric hydroxyapatite (HA) coating on TA6V substrate obtained by electrodeposition is presented. Based on special specimen preparation for STEM, this characterization under at the micrometer scale, shows that the HA coating presents a crystal size variation of about 75–300 nm from the coating surface to the coating/substrate interface, respectively. On the other hand, the use of two different electrolyte temperatures (40 and 65 °C) during the electrodeposition allowed us to obtain HA coatings with different microporosities. We believe that the electrodeposition process followed by a structural and chemical analysis may provide an effective means for fabricating bioactive calcium phosphate coatings on TA6V substrate at low temperatures. The main advantage of this technique is that the electrodeposition parameters can be easily controled, thus allowing the fabrication of calcium phosphate coatings which may be expected to be more beneficial to new bone growth during surgical implantation.

References

1. B. C. WANG, E. CHANG, T. M. LEE and C. Y. YANG, *J. Biomed. Mater. Res.* **29** (1995) 1483.
2. C. Y. YANG, B. C. WANG, E. CHANG and JD. WU, *ibid.* **6** (1995) 249.
3. M. SHIKHANZADEH, *J. Mater. Sci. Lett.* **10** (1991) 1415.
4. YONG HAN, KEWEI XU, JIAN LU and ZHU WU, *J. Biomed. Mater. Res.* **45** (1999) 198.
5. M. SHIKHANZADEH, *J. Mater. Sci. Mater. Med.* **6** (1995) 90.
6. T. A. HALL, *Phys. Tech. Bioch. Res.* **1a** (1971) 157.
7. P. LAQUERRIERE, V. BANCHET, J. MICHEL, K. ZIEROLD, G. BALOSSIER and P. BONHOMME, *Micros. Res. Tech.* **52** (2001) 231.
8. P. LAQUERRIERE, A. J. P. ALIX, G. BALOSSIER and P. BONHOMME, *Innov. Tech. Biol. Med.* **20** (1999) 27.

9. K. NAKAMOTO, ‘‘Infrared and Raman Spectroscopy of Coordination Compounds (fourth edition)’’ (Wiley-Interscience, New York, 1986) p. 36.
10. YONG HAN, KEWEI XU and JIAN LU, *J. Mater. Sci. Mater. Med.* **10** (1999) 243.
11. P. LAQUERRIERE, L. KILIAN, A. BOUCHOT, E. JALLOT, A. GRANDJEAN, M GUENOUNOU, G. BALOSSIER, P. FRAYSSINET and P. BONHOMME, *J. Biomed. Mater. Res.* **58** (2001) 238.
12. YONG HAN, TAO FU, JIAN LU and KEWEI XU, *ibid.* **54** (2000) 96.

Received 14 August 2001
and accepted 27 March 2002